ISSN 1343-2230

CNS-REP-24
August, 1999

CNS

CNS Report

Beam Emittance Measurements Using Alumina Screen at KCCH-MC50 Cyclotron

Shin-ichi Watanabe
Center for Nuclear Study, Graduate School of Science, University of Tokyo
3-2-1, Tanashi-shi, Midoricho, Tokyo, 188-0002, Japan

Jang-Ho Ha, Yu-Seok Kim, Hye-Young Lee and Jong-Seo Chai
Cyclotron Application Laboratory, Korea Cancer Center Hospital
Gongneung-Dong, Nowon-Ku, Seoul, Korea

Center for Nuclear Study(CNS)
Graduate School of Science, University of Tokyo
3-2-1 Midori-cho, Tanashi, Tokyo, 188-0002 Japan
Correspondence: cnsoffice@cns.s.u-tokyo.ac.jp

Beam Emittance Measurements Using Alumina Screen at KCCH-MC50 Cyclotron

Shin-ichi Watanabe
Center for Nuclear Study, Graduate School of Science, University of Tokyo
3-2-1, Tanashi-shi, Midori-cho, Tokyo 188-0002, Japan

Jang-Ho Ha, Yu-Seok Kim, Hye-Young Lee and Jong-Seo Chai
Cyclotron Application Laboratory, Korea Cancer Center Hospital
Gongneung-Dong, Nowon-Ku, Seoul, Korea

Abstract

The transverse beam emittance of the medical cyclotron KCCH-MC50 in Seoul was determined from measurements of the beam width on a profile monitor as an upstream quadrupole field is varied. The beam profile monitor system comprises the 99.5 % alumina with chromium oxide, an industrial TV camera, and an image data stored system. Using the stored data on the personal computer makes detailed analysis of the beam profile. The measured beam emittance derived from FWHM of the beam profile is a good agreement to the designed factory data. In this presentation, we describe the experimental setup, results, and conclusion of beam emittance.

1. Introduction

A transverse-beam emittance can be measured using the lattice optics of a transport line and a profile monitor located where the betatron sizes of the beam dominate. In an example of the quadrupole - drift - profile monitor method, a quadratic dependence of the beam width is given by

$$Y=A(k-B)^2+C \qquad (1)$$

Here Y is the square of beam width and k is $B'L/B\rho$ of an upstream quadrupole magnet. The coefficients of A, B, and C are obtained from the quadratic curve fit parameters.

The beam emittance E is given by

$$E = L^{-2}\sqrt{AC} \qquad (2)$$

where the factor L is distance between a center of quadrupole magnet and the fluorescence screen.

Various kinds of beam emittance monitor, which is based on the quadratic dependence of the beam width, have been developed for the electron machine. [1,2, and 3] These monitors feature the measurement of small emittance beam. The width of electron beam is sensitive to the strength of upstream quadrupole magnet (k-value control) because the electron mass is small compared with ions at the identical magnetic rigidity. This method is seemed to easy to measure the beam emittance of the electron beam because an electron gun provides unified beam structure like the single spot beam source. On the other hand, this method is seemed to difficult to measure the beam emittance of the multi-charged ion source because of complicated beam structure. Is it applicable to the large emittance beam such as the beam from the ECR ion source or the cyclotron ? The INS, University of Tokyo, had been tested the alumina screen using the 26 MeV Alpha beam [4] because the hardness and chemical property against the irradiated nuclear beam full fill the operating condition. The alumina screen, which is the one of the fluorescence screens, has still major contribution to diagnose a density, width, and center of the nuclear beam at the still low beam current below 10 pA. The Kyoto group developed the beam emittance monitor for the proton beam, where was measured by using the alumina screen at the kinetic energy of 50 KeV, 1 MeV, and 7 MeV [5].

The CNS-KCCH group has been promoting the development of the beam emittance monitor using the alumina screen, which had originally been proposed as the 2nd step of the monitor development following achievement of preliminary test at the sector focussing cyclotron (K=68) of Center for Nuclear Study, University of Tokyo. The measurement of beam emittance using the alumina screen was performed at the medical cyclotron KCCH-MC50 in Seoul (K=50). To measure the beam emittance, CNS group had provided the alumina screen, data acquisition board, and data acquisition software. In this presentation, we describe the beam profile monitor using the alumina screen, beam experiment, data analysis of measured profiles, calculation of beam optics, and the conclusion of beam emittance. Main contribution to the beam profile is an uncertainty of the ion source. The lack of uniformity and the incomprehensible behavior of the ion source are excluded in this presentation.

2. Experimental Setup

The KCCH-MC50 in Seoul, which was built by Scanditronix in 1986, is a variable energy isochronous cyclotron for acceleration of light ions. The layout of a KCCH-MC50 cyclotron facility is illustrated in Fig. 1. The parameters of KCCH-MC50 are tabulated in Table 1. The beam transport line comprises a switching magnet, a quadrupole magnet family, a gantry system, and beam diagnostic devices. A switching magnet is used to deliver the beam to the room where is a gantry room, a target room, and a RI room. The beam diagnostic devices are located at the exit of cyclotron, the exit of first triplet quadrupole magnets, the exit of the switching magnet, and the exit of third triplet quadrupole magnets, respectively. The slit and steering system are provided for the adjustment of the beam center. The cyclotron vault is separated with radiation shield. The plug system with a carbon shield is located in the beam transport line to protect the neutron radiation from the cyclotron vault. The present gantry system provides a straight beam course where is utilized for the beam application such as the test of beam monitor like the fluorescence screen described in this paper. The exit of the straight beam course is designed as an isocenter of the beam transport line.

The experimental setup for the emittance measurement is shown in Fig. 2, where the alumina screen is located at the down stream of the last quadrupole magnet named QU8. The distance between the exit of cyclotron (P_1) and the alumina screen (P_2) is 15.752 m long. The distance between the center of QU8 and the alumina screen is of 5.164 m. The last quadrupole magnet, QU8, is the middle of quadrupole-triplet. The last of quadrupole-triplet is excluded to play the role of drift space in the beam line. So the quadrupole – drift – profile monitor structure is realized. The quadratic dependence of the beam width was measured with the alumina screen.

Alumina is promising for high melting point material under nuclear beam irradiation because it's high hardness and high chemical stability. The alumina screen used in this experiment comprises Al_2O_3+CrO_3 plate of AF995R (Desmarquest) with 1-mm thickness. The doped oxide chromium plays a role of fluorescence source. The light spectrum from the AF995R is expected around 700 nm. Physical characteristics of the AF995R are tabulated in Table 2. The effective area of alumina screen is designed at 888 mm^2 but the physical sizes of alumina screen are 50x50 mm^2.

The schematic view of the screen monitor is shown in Fig. 3. The alumina screen is installed in a cubical vacuum chamber of the screen monitor. The side wall of the vacuum chamber is provided for a view port with a crystal glass of 60 mm-ID. The

alumina screen was fixed on a movable rod, which is inserted in the vacuum chamber, with an angle of 45 degree to the beam direction. The beam profile on the alumina screen can be observed through the view port. The vacuum chamber was evacuated up to 10^{-6} Torr with a turbo molecular pumping system.

An industrial TV camera (ITV) is placed at the gantry room as shown in Fig. 2. An iris control is made to adjust the light flux reached at the image tube. The room light in the gantry room is turned off to suppress the background noise on the ITV signal. An image tube of the ITV is of monochrome type because of the radiation resistance. The signal processing system is illustrated in Fig. 4. The beam profile signal is based on the NTSC standard and is connected to an IBM type PC. The IBM type PC captures a beam profile signal with the aid of an image processing circuit (AIMS GrabIT Pro) which is the one of the data acquisition boards. An amplitude resolution of the ADC in the image processing circuit is 8-bit. The digitized beam profile signal is stored in a graphic memory as a beam profile data. The beam profile data in the graphic memory is saved onto the hard disc for later detailed study. The size of the beam profile data stored in the hard disc is chosen at 910 KB with a bitmap format (BMP). The beam profile data in the graphic memory are displayed simultaneously on the monitor TV. To show the series of captured beam profiles, eight pictures are displayed on the monitor TV at once with the aid of a sum-nail function of the image data processing circuit. It is remarked that the sensitivity of the image tube used in the ITV is assumed at γ=1. The image-processing tool enable us the correction of the value, γ, when the analysis of the beam width has been done.

3. Experiments and image data processing

The experiment was performed using a 50.5 MeV proton beam. The beam current measured with the faraday cup was 1.5 nA. First, width of the beam irradiated on the alumina screen was adjusted so that the fluorescence was contained within an effective area of the alumina screen. Subsequently, the excitation current of QU8 was chosen at 18.1 A to make a circular beam profile, which was found near the bottom of the quadratic curve fit, on the associate alumina screen. Then the excitation current of QU8 was changed to measure k-value dependence of the beam profile data. The beam profile data appropriate for the calculation of beam emittance are saved on the hard disc after the change of excitation current. Some samples of measured beam profiles are shown in Figs. 5-1, 2 and 3, respectively when the excitation current of QU8 was chosen at 18.1, 15.1 and 21.1 A respectively.

The beam profile data saved on the hard disc were analyzed by using the image-processing tool in order to measure the beam sizes on the alumina screen. A difficulty of the image data processing is mathematical processing such as a subtraction of noise signal from the measured beam profile data. The brightness and quality of the measured beam profile are influenced by the noise signal, unavoidable beam hallo, and time structure from the ion source.

The image-data processing tool offers the function to show the three dimensional (3D) data in X, Y, and Z coordinates. Fig. 6 shows the 3D display of the beam profile data as shown in Fig. 5-1. The axis X and Z shown in Fig. 6 represent the two-dimensional coordinates associate with a surface of the alumina screen plate. The axis Y represents the beam intensity. In Fig. 6, the top of contour map is recognized as a center of beam profile irradiated on the alumina screen. The tail noise in the beam profile is taken into account the systematic error of the associate beam width.

The pixel number in the beam profile data gives the beam intensity irradiated on the alumina screen. For example, Fig. 7 shows that the X and Y-axis represent the pixel number and the beam intensity, respectively. On the other word, the X-axis represents a radial direction of the transported beam. A spectrum height, which is the beam intensity, is a projection of the pixel data along the Z-axis. We can calculate the beam size by using the digital scale function supported by the image-processing tool. The tail noise and a fluctuation of the spectrum are to be subtracted from the original data when a calculation of the beam emittance. Various definitions of the beam width are in use to calculate the beam emittance. We discuss here the Gaussian distribution associate with the beam width of the standard deviation σ. The full width at half maximum (FWHM) and the full width at 90 % maximum are discussed in the following section.

4. Discussions

4-1 Beam condition

The beam emittance measurement has been done under the following boundary conditions; the fluorescence due to the irradiation of the nuclear beam is proportional to the beam current; the light intensity of the fluorescence is not decreased by experiences of the medium between the alumina screen and the focussing point of the ITV camera; the dynamic range of the sensitivity to the light flux is infinitive.

A saturation level of the alumina screen is considered to evaluate the dynamic range of the alumina screen to the irradiation level of the nuclear beam. A linearity of the fluorescent flux to the irradiated beam current is estimated. An estimated beam

current excess 250 nA/cm^2 irradiated to the alumina screen deteriorate a linearity of fluorescent flux. This estimation is derived from the preliminary test using a 26 MeV Alpha beam from the sector focussing cyclotron of Institute for Nuclear Study, University of Tokyo [4]. The beam current of 1.5 nA was chosen at the experiment using the KCCH-MC50 cyclotron. We assumed that the beam density is flat in the irradiate area and the beam current is constant during the beam profile measurement. Thus, the estimated beam intensity is 47.8x10^7 e/mm^2 s as the beam current is 1.5 nA. A recommended lifetime, which is an integrated beam intensity to the unit area, of the alumina screen is 1x10^{18} e/mm^2. The estimated beam density is 2.5x10^7 e/mm^2 s at the beam sizes of 25 x 15 mm^2 on the associate alumina screen. A threshold level from the view point of the excitation of the fluorescence is 1x10^{7}e/mm^2 s. So the beam sizes above mentioned are acceptable area at the beam current of 1.5 nA.

If the lack of data due to a timing coincidence is existed in the measurement system, signal conditioning circuit is to be used in the experimental setup. We have had considered the synchronization of the beam profile to the image data processing circuit. The cyclotron beam gives bunching structure due to the given energy from the Dee of the cyclotron. A decay time of the fluorescence emitted from the alumina screen is estimated at 3 x 10^{-3} sec. We could say that the time periods of the cyclotron bunched beam is faster than this decay time. This means that the lack of beam profile data is not occurred during the irradiation of the beam on the alumina screen.

4-2 Beam optics and beam width

To estimate the beam width, using the computer has done the beam transport simulation [6]. In the calculation, the twiss parameter at the exit of KCCH-MC50 is assumed that βx=1.534 m, βz=3.303 m, αx=0.2138, and αz=0.6883, where is derived from the designed factory data of KCCH-MC50. The designed factory data is 4.2 mm, 2.8 mrad, and 11.5 π-mm mrad for *X*, *X'*, and *Ex*, respectively. The designed factory data is also 6.8 mm, 2.5 mrad, and 14 π-mm mrad for *Z*, *Z'*, and *Ez*, respectively. For convenient, dispersions ηx=0.73 m and ηz=0 m, $\eta x'$=0 and $\eta z'$=0, where is the reference of K68-SF cyclotron at CNS, U-Tokyo, is taken into account the estimation of the beam envelopes. Using these parameters, the beam width at the alumina screen has been calculated as the upstream QU8 current is varied. The calculated beam envelopes are shown in Fig. 8. The beta functions and dispersion functions (twiss parameter) of the beam transport line are shown in Fig. 9. Figs. 8 and 9 show the example of the beam optics in case of the upstream current QU8 current is 18.1 A.

The k-value dependence of the measured beam width, which is full width at 90 %

maximum, is tabulated in Table 3. Consequently, we gave the beam width of 11.3 mm in X-direction and the beam width of 13.05 mm in Z-direction, respectively. These values are not agreement to the calculated beam width. We should note that the beam profile monitor does not cover the exact beam width at 90% maximum because the beam acceptance of the transport line is small compared with expected acceptance area. Unfortunately, the beam is prevented with the slit element located at the upstream of the profile monitor in the beam transport line. Then the true k-value dependence could not be measured because the tails of the spectrum, which was involved in the full width at 90 % maximum, was disappeared by prevention of the transported beam.

The quadratic dependence of the beam width, which is defined by the FWHM, is tabulated in Table 4. The measured beam width as a function of k-values is shown in Fig. 10. In the Fig. 10, the curve fit lines of the square of the beam width, Yx and Yz, are shown.

4-3 Beam emittance

The beam emittances Ex and Ez are given by the equations (1) and (2), respectively. The coefficients, A and C, are derived from the quadratic equation of beam width, Yx and Yz, in the Fig. 10. The parameter L is 5.164 m between P1 and QU8 as shown in Fig. 2. The beam emittance calculations give the values of Ex = 7.5 and Ez = 10.3 π-mm mrad, respectively. These emittances are fairly good agreement to the designed factory data of 11.5 and 14 π-mm mrad, respectively. On the other hand, we should note that the difference between the designed factory data and the measured beam emittance Ex of 21.4 π-mm mrad, for example, which was derived from the full width at the 90 % maximum.

The reason is discussed as follows; the parameter A in the equation (1) mentioned in the previous section, depend on the quadratic force influenced by the upstream quadrupole magnet QU8; the parameter A represents the $\sigma_o^2 R_{12}^2$, where the σ_o and R_{12} are the beam size in the upstream quadrupole magnet of strength k and the transfer matrix element between the quadrupole and the alumina screen, respectively. In the equation (1), the parameter B represents the k_0 where is the quadrupole strength at the minimum of the parabola. The parameter C represents the $\varepsilon^2 R_{12}^2/\sigma_o^2$. If the parameter σ_o is influenced by any reason at the upstream of QU8, we could not determine the precise beam width at the alumina screen.

The detailed discussion is found [2]. The measured beam emittance ε_m is given by,

$$\varepsilon_m = \sqrt{\frac{\sigma_o^2 \sigma_{sys}^2}{R_{12}^2} + \varepsilon_r^2} \qquad (3)$$

where the σ_{sys} and the ε_r are the system resolution and the actual beam emittance, respectively.

The system resolution, σ_{sys}, is good in the present experiment because of 8 bit resolution of ADC in the image processing circuit. Then the first term in the square root becomes small values compared with actual beam emittance, ε_r. Thus the measured emittance becomes near ε_r. The beam width derived from the FWHM is not including the tails region of density distribution where is prevented by the insertion devices such as the slit and collimator. So, the calculation of the beam emittance using the FWHM gave the actual beam emittance.

5. Summary

The quadratic dependence of the beam width was measured at the KCCH-MC50 cyclotron. The summary is as follows: We show the beam profile data measured with the alumina screen, Al_2O_3+CrO_3 plate of AF995R (Desmarquest) with 1-mm thickness. The extracted beam current is 1.5 nA protons at 50.5 MeV. The beam profile was measured with ITV camera system and was analyzed with the image processing tool. The beam profile data was evaluated to determine the transverse beam emittance according with both the projections where the full width at 90 % maximum and the FWHM. The measured beam emittance based on the beam width of FWHM is a good agreement to the designed factory data of Ex = 11.5 and Ez = 14 π-mm mrad, respectively.

6. Acknowledgments

The authors wish to thank the cyclotron crew of the KCCH-MC50 cyclotron application laboratory for their helpful operation. The first author thanks Prof. Y.Shida for his valuable comments and discussions. This work was supported in part by grant-in-aid for Joint Research Project under The Japan-Korea Basic Scientific Promotion Program (KOSEF-JSPS).

References

[1] M. C. Loss *et al.*, "Automated Emittance Measurements In The SLC",SLAC-PUB-4278, March 1987 (A)

[2] M. C. Loss *et al.*, "High Resolution Beam Profile Monitors In The SLC", Transaction of Nuclear Science, Vol.NS-32, No.5, Oct. 1985.

[3] Y. Hashimoto *et al.*,"Beam Profile Monitor Using Alumina Screen And CCD Camera" INS-T-511, Aug. 1992.

[4] S. Watanabe *et al.* "Beam-Profile Measurement with an Al_2O_3+Cr Plate", Annual Report 1994, INS Tokyo-University, pp25-26.

[5] T. Shirai *et al.*, "Emittance Monitor With View Screen And Slits", Proc. of Linac'94, Japan, 1994.

[6] Phil Bryant, CERN, private communication, http://nicewww.cern.ch/~bryant

Table 1. The Characteristics and Specifications of MC 50 Cyclotron

General

Accelerating particles	Energy	Beam intensity
P	20 ~ 50 MeV	60 μA
d	10 ~ 25 MeV	30 μA
α	25 ~ 52 MeV	30 μA
He - 3	20 ~ 70 MeV	20 μA

Magnet system

Pole diameter	143 cm
Minimum gap	11 cm
Maximum gap	19.7 cm
Sectors number	3
Spiral angle in degrees	max. 55
Circular trim coils	10 pairs
Maximum average field	17.5 kG
Minimum average field	10.5 kG
Maximum hill field	20.5 kg
Magnet field stability	1×10^{-5}

RF system

Dees	2
Width in degrees	90°
Minimum aperture	2.0 cm
Frequency range	26.8 to 15.5 MHz
Frequency stability	10^{-6}
Dee tuning by movable short, mode	λ/4
Dee voltage (maximum)	40 kV
Dee voltage stability	$< 10^{-3}$

Table 2. Specifications of the fluorescence screen

Main Constitution	99.5% Al_2O_3 (Activator Cr)
Melting point	1850 C.D
Absolute density	3.98
Coefficient of thermal expansion	$8.6x10^{-6}$
Specific heat 20 < T < 1000 C.D	1.09 J/cm.s.C.D
Dielectric strength	30-35 kV/mm
Electric resistively	$10^{14}\Omega$/cm
Relative sensitivity	$1x10^{7}$ e/mm^2.s
Lifetime	$1x10^{18}$ e/mm^2

Table 3. K-value dependence of the measured beam width (90% maximum)

K m^{-2}	K*L m^{-1}	Yx-90% pix	Yz-90% pix	Yx-90% mm	Yz-90% mm	(Yx/2)^2 mm^2	(Yz/2)^2 mm^2
4.931	0.73965	103	163	20.6	32.6	106.09	265.69
5.117	0.76755	84	127	16.8	25.4	70.56	161.29
5.178	0.7767	80	106	16	21.2	64	112.36
5.238	0.7857	77	101	15.4	20.2	59.29	102.01
5.3	0.795	71.5	80.5	14.3	16.1	51.1225	64.8025
5.42	0.813	63	61	12.6	12.2	39.69	37.21
5.48	0.822	56.5	65.25	11.3	13.05	31.92	42.575
5.54	0.831	50	60	10	12	25	36
5.602	0.8403	54.5	60.5	10.9	12.1	29.7025	36.6025
5.663	0.84945	54	60	10.8	12	29.16	36
5.72	0.858	55	63	11	12.6	30.25	39.69
5.84	0.876	69	69	13.8	13.8	47.51	47.61
5.965	0.89475	86	78	17.2	15.6	73.96	60.84
6.025	0.90375	98	80	19.6	16	96.04	64
6.328	0.9492	172	92	34.4	18.4	294.84	84.64

Table 4. K-value dependence of the measured beam width (FWHM)

K m^{-2}	K*L m^{-1}	Yx-FWHMpix	Yz-FWHMpix	Yx-FWHM mm	Yz-FWHM mm	$(Yx/2)^2$ mm^2	$(Yz/2)^2$ mm^2
4.931	0.73965	71	124.5	14.2	24.9	50.41	155
5.117	0.76755	49	76	9.8	15.2	24.01	57.76
5.178	0.7767	50	66	10	13.2	25	43.56
5.238	0.7857	50.5	64.5	10.1	12.9	25.5	41.6
5.3	0.795	47	49	9.4	9.8	22.09	24.01
5.42	0.813	40.5	36	8.1	7.2	16.4	12.96
5.54	0.831	34	34	6.8	6.8	11.56	11.56
5.602	0.8403	34	34	6.8	6.8	11.56	11.56
5.663	0.84945	32.5	36.5	6.5	7.3	10.563	13.3225
5.72	0.858	33	38	6.6	7.6	10.89	14.44
5.84	0.876	34	44	6.8	8.8	19.36	11.56
5.965	0.89475	44	56	8.8	11.2	31.36	19.36
6.025	0.90375	68	58	13.6	11.6	46.24	33.64
6.328	0.9492	112	78.5	22.4	15.7	125.44	61.6225
6.449	0.967	118	93	23.6	18.6	139.24	86.49

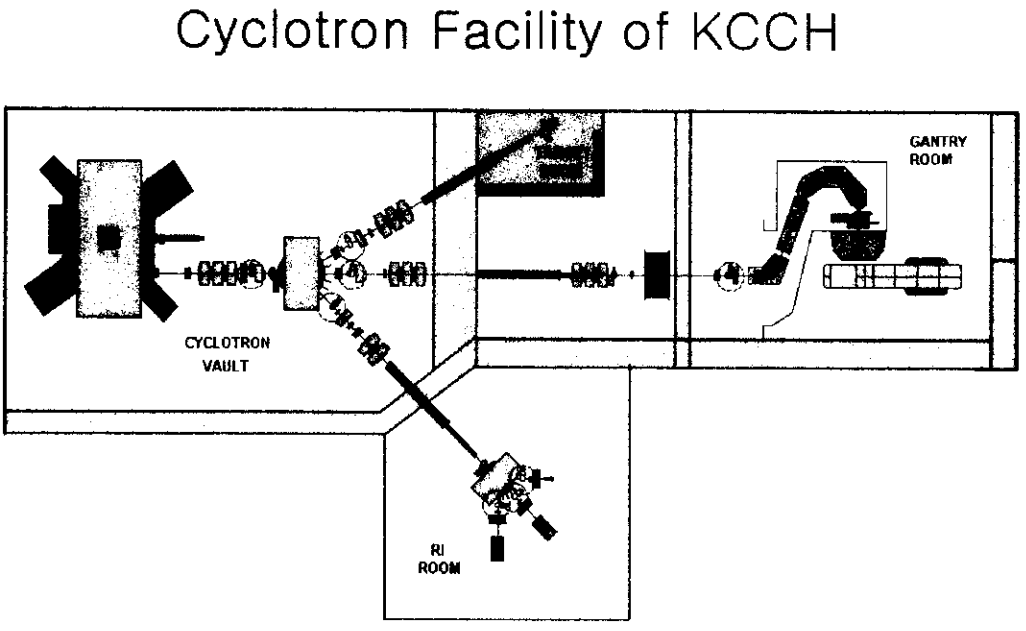

Fig. 1. Layout of KCCH-MC50 cyclotron facility. Alumina screen is located at the end of beam course in the gantry room.

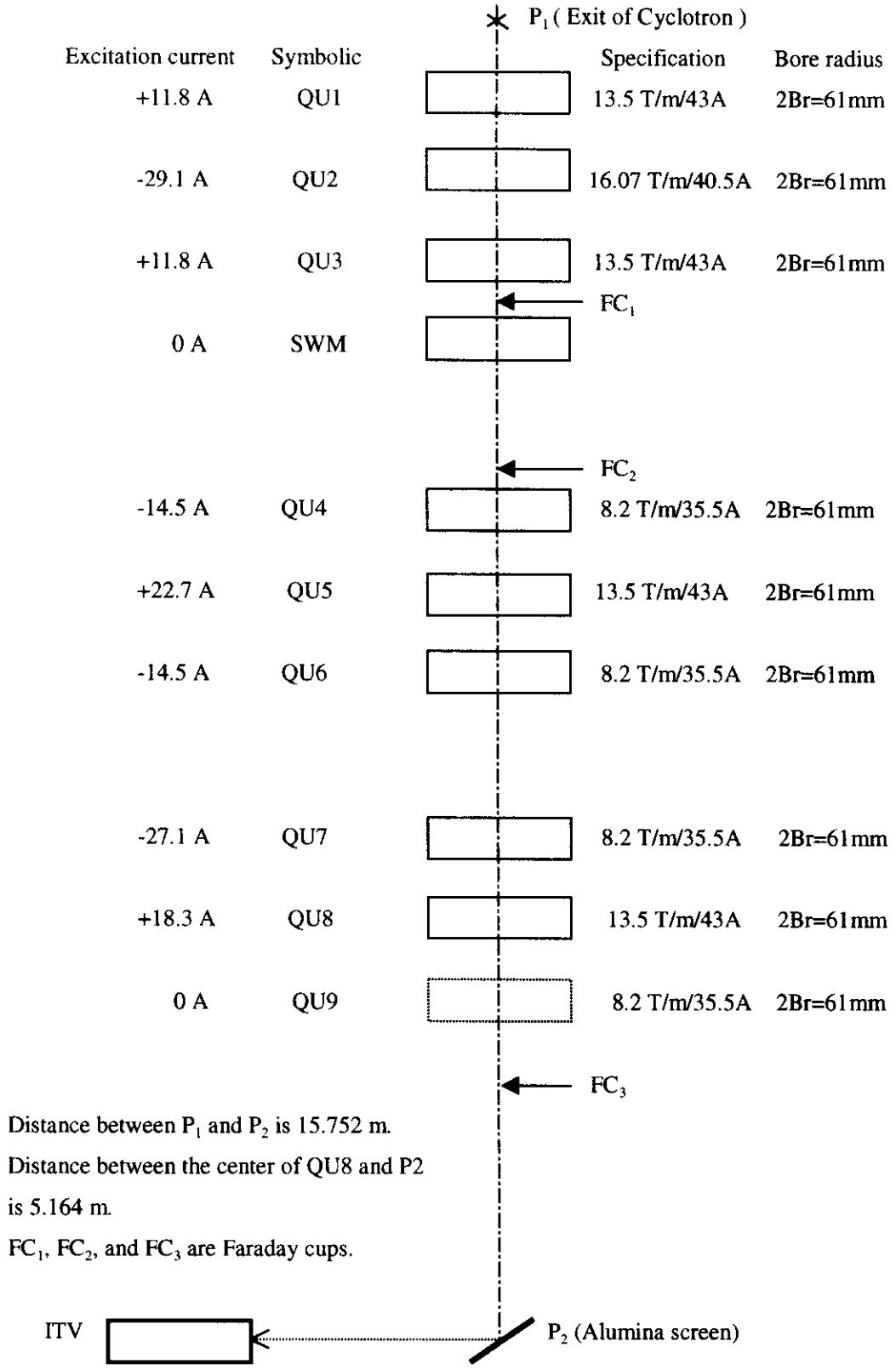

Fig. 2. Experimental set up of the beam transport line at the KCCH-MC50 treatment course.

Side view

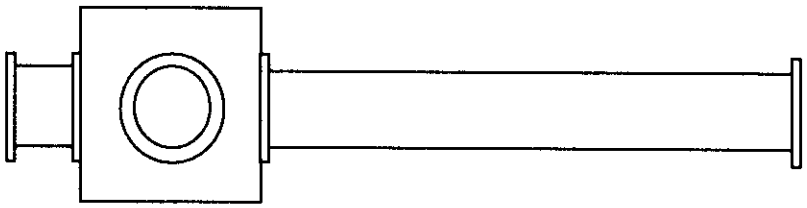

Upper view (cut in half)

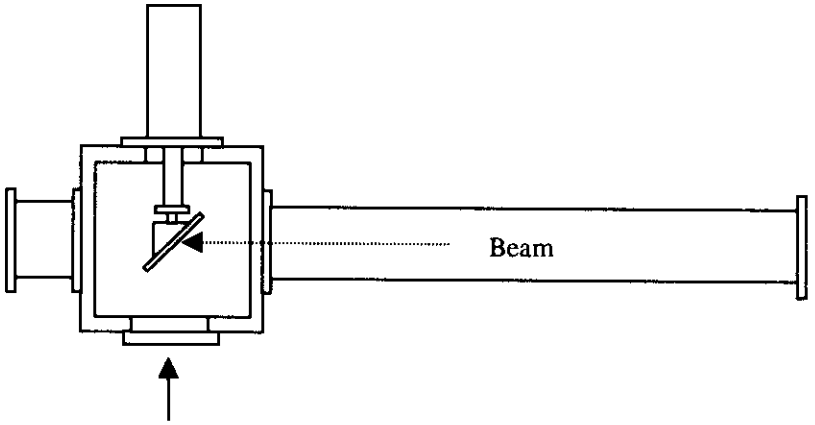

Fig. 3. Schematic view of the screen monitor

Fig. 4. Schematic of image data processing system.

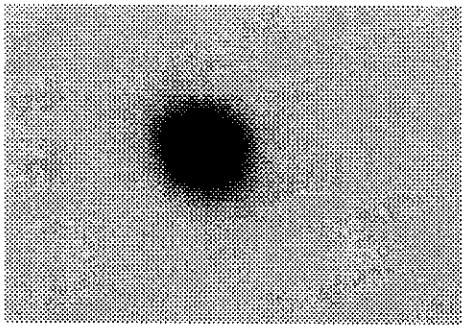

Fig. 5-1. Measured beam profile at QU8=18.1A

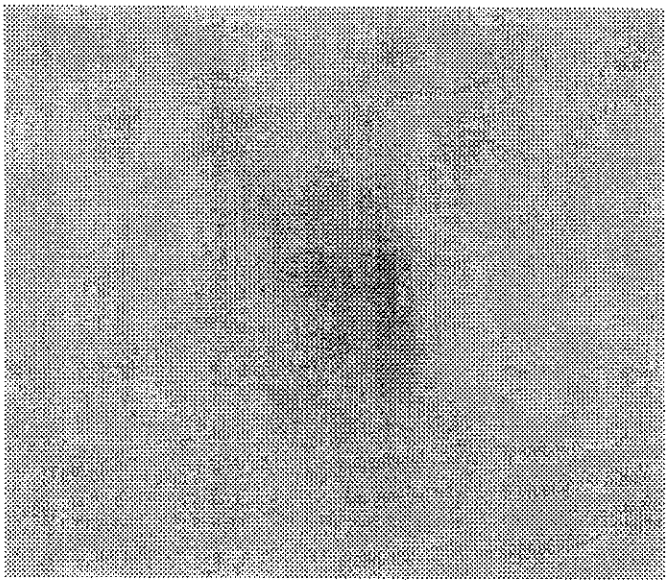

Fig. 5-2. Measured beam profile at QU8=15.1A

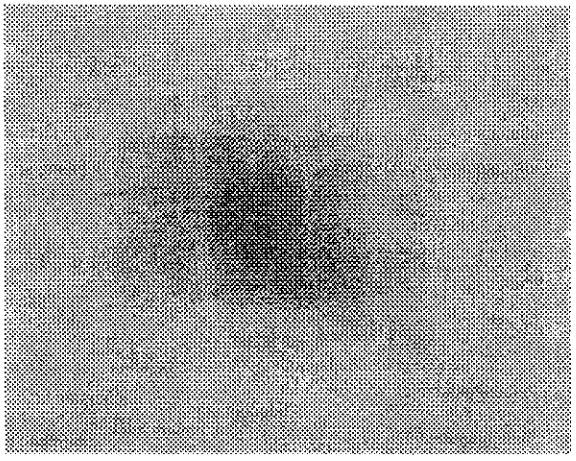

Fig. 5-3. Measured beam profile at QU8=21.1A

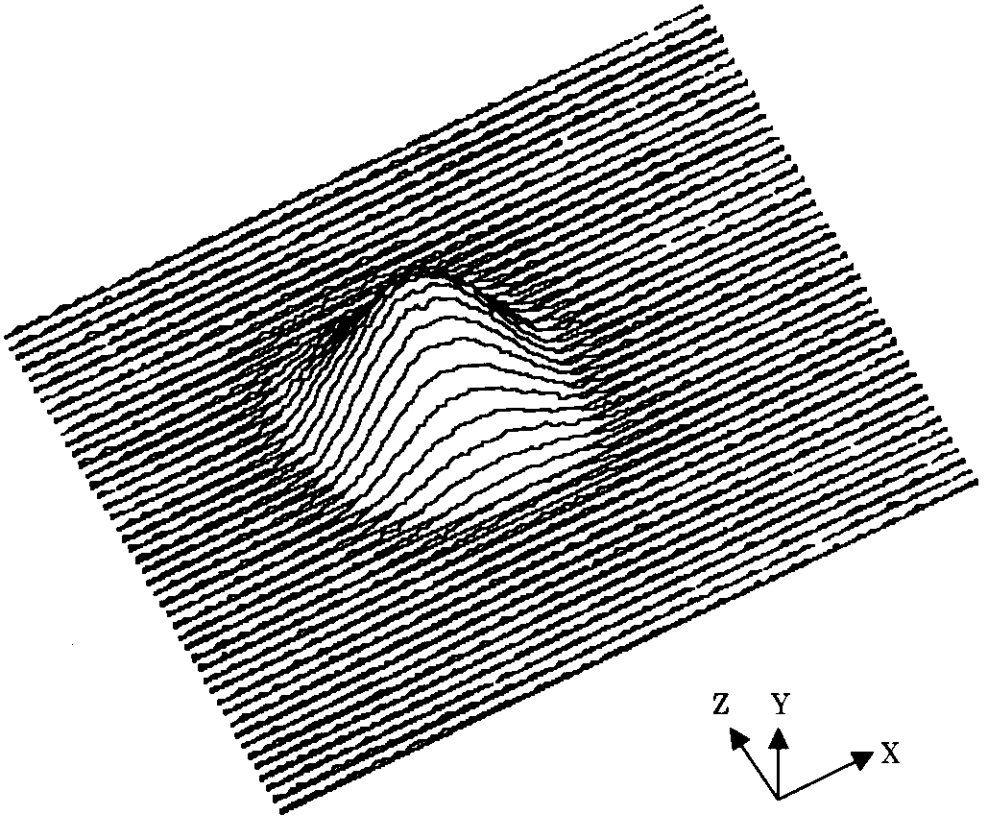

Fig. 6. 3D projection of measured beam profile at QU8=18.1 A.

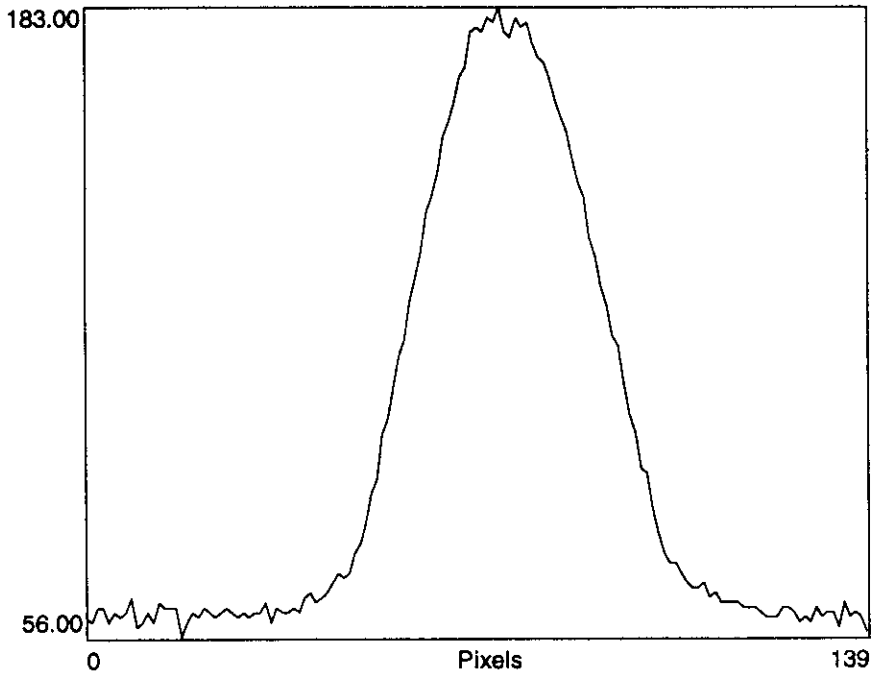

Fig. 7. X-Y projection of measured beam profile at QU8=18.1 A.

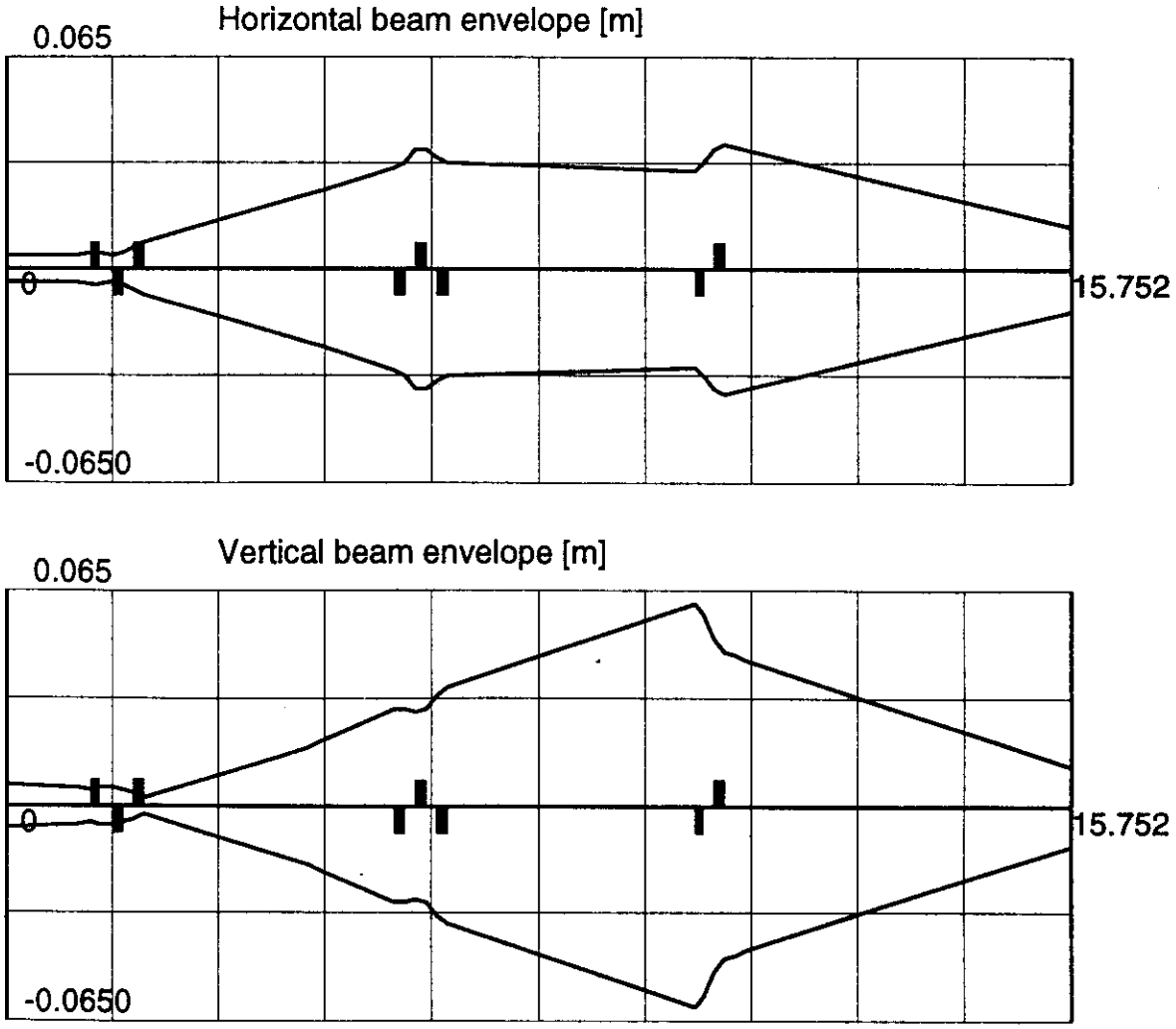

Fig. 8. Calculated beam envelopes of KCCH-MC50 transport line modified for the emittance measurement. Upper and lower show the beam envelopes in the horizontal direction (x-coordinate) and in the vertical direction (y-coordinate), respectively.

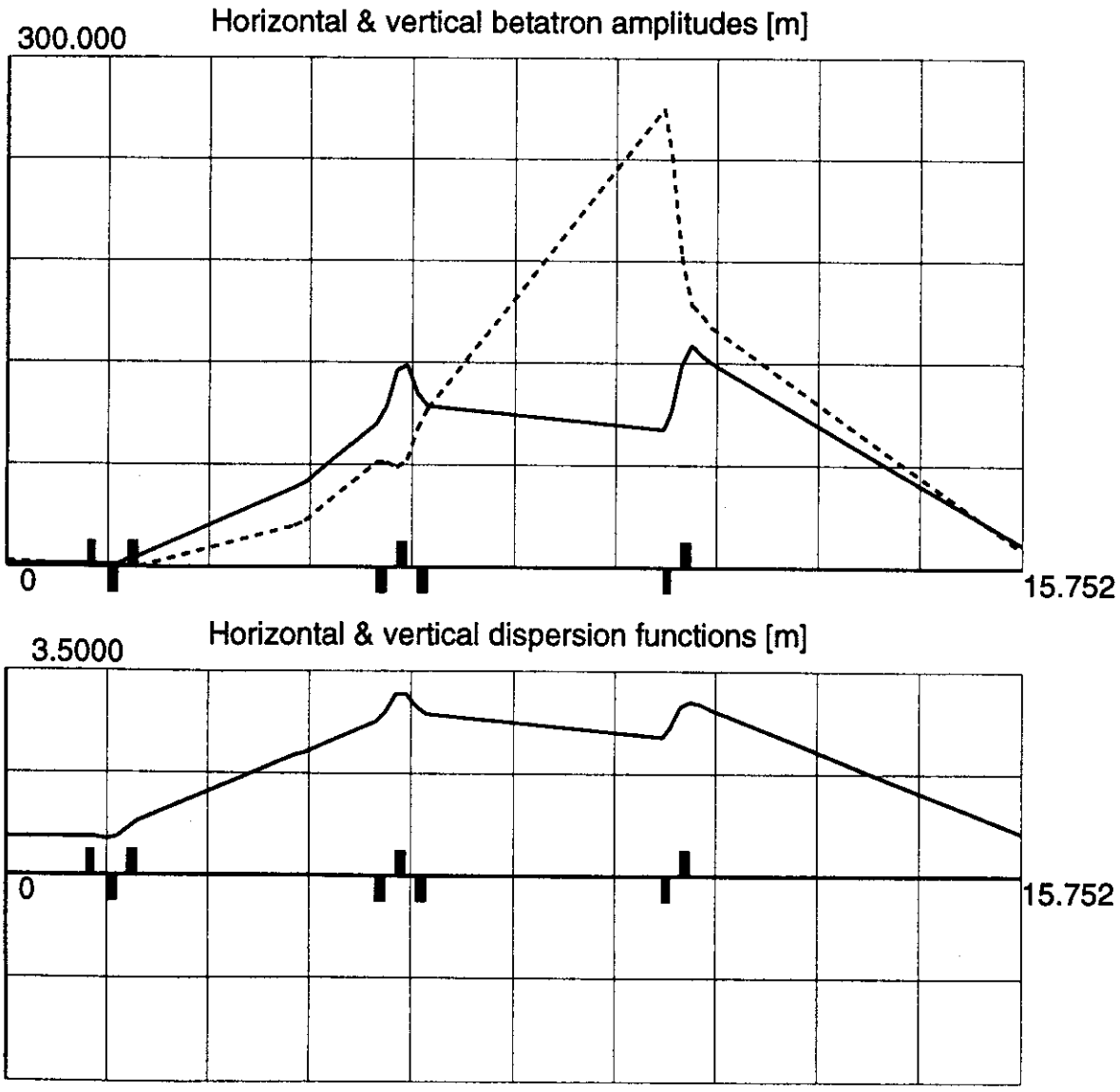

Fig. 9. Twiss parameters of the KCCH-MC50 transport line at the experimental setup. Upper and lower show the vertical and horizontal beta functions and the dispersion functions, respectively. The left and the right represent the exit of cyclotron (P_1) and the center of alumina screen (P_2), respectively.

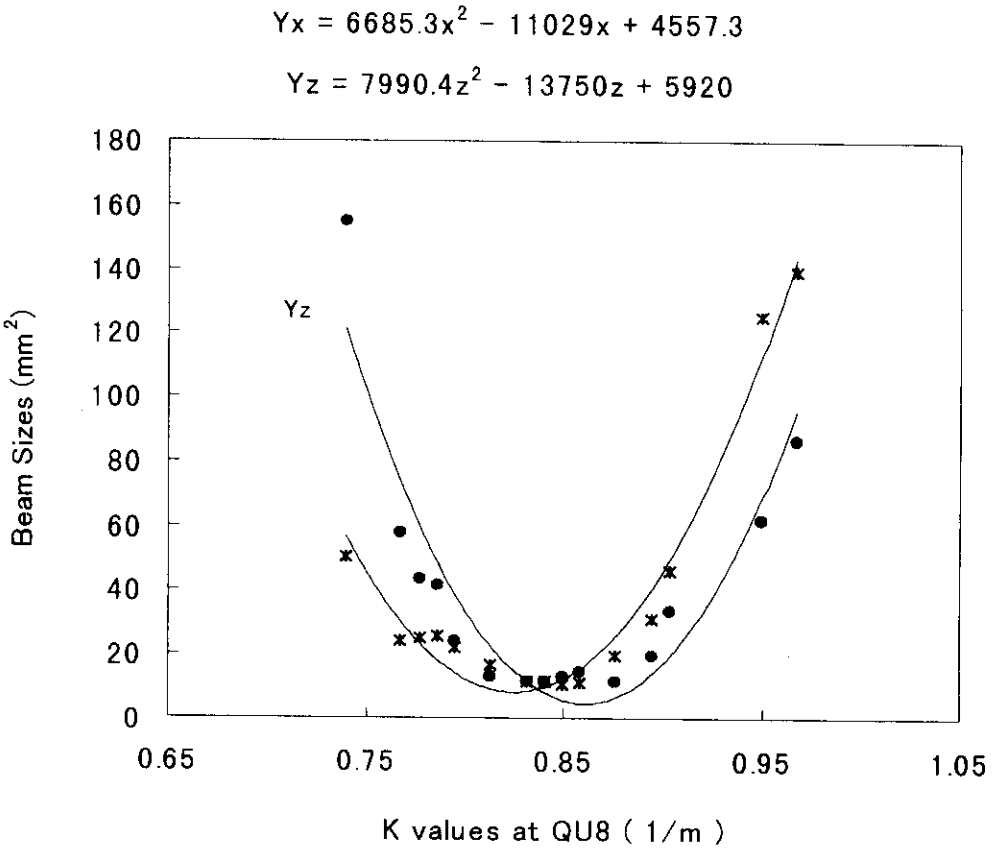

Fig. 10. K-Value dependence of the measured beam width (FWHM)